

Received March 2, 2017, accepted March 24, 2017, date of current version June 28, 2017.

Digital Object Identifier 10.1109/ACCESS.2017.2705146

Performance Analysis of Distributed MIMO With ZF Receivers Over Semi-Correlated \mathcal{K} Fading Channels

XINGWANG LI^{1,2}, XUEQING YANG¹, LIHUA LI², JIN JIN³, NING ZHAO¹, AND CHANGSEN ZHANG¹

¹School of Physics and Electronic Information Engineering, Henan Polytechnic University, Jiaozuo 454000, China

²State Key Laboratory of Networking and Switching Technology, Beijing University of Posts and Telecommunications, Beijing 100876, China

³School of Information and Engineering, Zhengzhou University, Zhengzhou 450001, China

Corresponding author: Lihua Li (lilihua@bupt.edu.cn)

The work was supported in part by the National Science and Technology Major under Project 2015ZX03001034, in part by the Doctoral Scientific Funds of Henan polytechnic University under Grant B2016-34, in part by the Open Research Fund of State Key Laboratory of Networking and Switching Technology, BUPT, under Grant SKLNST-2016-1-02, and in part by the National Natural Science Foundation of China under Grant 61501404, 41604112.

ABSTRACT Distributed multiple-input multiple-output (D-MIMO) systems have drawn considerable attention as they can combine the advantages of point-to-point MIMO with distributed antenna system (DAS). However, the performance analysis of D-MIMO system with zero-forcing (ZF) receivers over semi-correlated \mathcal{K} fading channels involves special functions, such as Bessel and Meijer-G functions, which do not enable us to further analysis. In this paper, by using moment matching method, we present a new method that use a Gamma distribution to approximate the \mathcal{K} distribution (Rayleigh/Gamma distribution). Using the approximate distribution as a starting point, we derive the approximate analytical expressions on the achievable sum rate (ASR), symbol error ratio (SER), and outage probability (OP) of D-MIMO systems operating in semi-correlated \mathcal{K} fading channels employing ZF receivers. To get useful insight into implications of system and fading parameters on the performance, the analytical asymptotic approximations on the ASR in high signal-to-noise ratio (SNR) and low-SNR regime are provided, respectively. Finally, we perform the approximate large-system analysis in the high-SNR and provide asymptotic sum rate expressions when the number of antennas at the base station (BS) grows large, and when the number of antennas at both ends grows large with a fixed and finite ratio. It is demonstrated that the proposed approximate expressions accurately match with the analytical expressions, especially for large-system limit.

INDEX TERMS Distributed multiple-input multiple-output, massive MIMO, \mathcal{K} fading channel, moment matching method, zero-forcing receiver.

I. INTRODUCTION

Distributed multiple-input multiple-output (D-MIMO) system, which incorporates the advantages of conventional MIMO and distributed antenna systems (DAS) to obtain spatial multiplexing gains and macro-diversity gains simultaneously, has drawn considerable attention due to the significant growing demand for high data rate services [1]–[4]. These gains can be obtained by deploying multiple antennas at the radio access ports (RAPs) that are geographically distributed. However, different RAPs of D-MIMO system suffer from different path-loss and shadowing fading (a.k.a large scale fading) in view of different propagation paths and distances. This makes the performance analysis of D-MIMO system on the sum rate, symbol error rate (SER), and outage probability

a cumbersome problem. It is noteworthy that large scale fading is a crucial factor since it can significantly diminish the benefits of D-MIMO systems. For this reason, we herein investigate the performance of D-MIMO system over composite fading channels.

In the context of composite fading channels, Rayleigh/Log-Normal (RLN) composite fading model is known as a prevalent fading model, which is widely used to characterize the effects of composite fading in wireless and satellite communication channels [5], [6]. However, the composite probability density function (PDF) of RLN composite fading model is not in closed-form which hampers to further analysis. To circumvent this problem, Rayleigh/Gamma composite fading model which is dubbed \mathcal{K} fading model,

is introduced to model scattering in MIMO and radar environment [7], [8]. As for \mathcal{K} fading model, the Log-Normal distribution of RLN is approximated by the analytically friendlier Gamma distribution. Empirical measurements reveal that the Gamma distribution sufficiently models the shadowing fading and closely approximate the Log-Normal distribution [9], [10]. The main drawback of \mathcal{K} model is that the analytical expressions of achievable sum rate, symbol error ratio (SER), and outage probability performance involve special functions, such as Bessel, Meijer-G, and hypergeometric functions, which hamper further analytical derivations.

Motivated by the aforementioned discussion, we study the approximate performance of D-MIMO systems with semi-correlated \mathcal{K} fading channels with ZF receivers by using moment matching method. Herein ZF receivers are adopted for the following reasons: i) ZF receiver can eliminate the interference between antennas of the transmitters; ii) ZF receivers induces lower complexity compared to other receivers, such as successive interference cancellation (SIC) or minimum mean-squared error (MMSE); iii) it is convenient for analytical performance evaluation with ZF receivers. To the best of authors' knowledge, there are relatively few relevant works published in [3], [4], and [11]–[15]. In [3], the analytical expressions for upper and lower bound of ergodic capacity of D-MIMO systems with \mathcal{K} fading channels are derived, while based on the moment matching method, the approximate performance is not involved. Besides, the correlation and ZF detection are not taken into account in [3], whilst the two key metrics of symbol error ratio (SER) and outage probability (OP) are not considered either, which are used to characterize the performance for the cases of post-modulation and non-ergodic channels performance, respectively. In the similar case, [4] presents the approximate upper bound for the ergodic capacity of D-MIMO systems with generalized- \mathcal{K} fading channels using the moment matching method, yet the correlation, SER, OP and \mathcal{K} fading channels are not considered. Gore *et al.* [11] consider a point-to-point MIMO system operating in correlated Rayleigh fading, while the effects of shadowing and path-loss are not taken into account. In [12] and [13], the performance of D-MIMO system over \mathcal{K} fading channels is investigated, yet the derived expressions involve Bessel and Meijer-G functions, which hinder us to further analyze the effect of fading parameters. Ho and Stuber [14] and Al-Ahmadi and Yanikomeroğlu [15] use a single distribution function to approximate the composite function by matching mean and variance, while the analysis is performed for point-to-point MIMO system rather than D-MIMO system. Unfortunately, [3], [12], [13] do not yield engineering insights for practical system design, and large-scale MIMO, which is known as a disruptive technology for the fifth (5G) generation cellular networks [16]–[19], is not considered in [11]–[15] either. In this paper, we derive closed-form approximate expressions on the achievable sum rate, SER, and outage probability of D-MIMO system by using the derived approximate distribution function. In addition,

we investigate the asymptotic behavior for high and low signal-to-noise (SNR) regimes, respectively. Finally, the asymptotic performance of large-system limit on the achievable sum rate is also studied at the high SNR.

The contributions of this paper are summarized as follows:

(1) We deduce approximate PDF of a Gamma distribution to approximate the composite distribution with the aid of moment matching method, which is extensively used to approximate analysis for wireless communication systems [4], [20].

(2) Capitalize on the derived approximate PDF, we commence to derive the approximate expressions on sum rate, SER, outage probability in closed-form of D-MIMO systems over semi-correlated \mathcal{K} fading channels. These approximate expressions tighten across the entire SNRs and when the number of base station (BS) antennas grows large. More importantly, the proposed approximations provide engineering insights into the impacts of system and fading parameters on D-MIMO performance for integer parameters.

(3) In order to get intuitive insights into the impact of system parameters on the sum rate, we perform the asymptotic analysis at the high and low SNR regimes. In the high SNR regime, it is demonstrated that the approximate result approaches the analytical sum rate for high SNR and when the number of BS antennas grows large. In the low SNR regime, we explore the asymptotic sum rate by two metrics of the minimum energy per information bit to reliably convey any positive rate and the wideband slope.

(4) With the aid of the proposed sum rate, we investigate the asymptotic sum rate of large-system limit under the cases of fixed average transmit power and fixed total transmit power. It is demonstrated that the proposed approximate expressions on the sum rate match the theoretical results very well.

This paper will proceed as follows: Section 2 describes the D-MIMO fading channel model and presents the performance on the achievable sum rate, SER, and outage probability of D-MIMO system over the semi-correlated \mathcal{K} fading channel employing ZF receivers. The approximate PDF is derived by matching mean and variance in Section 3. In Section 4, we provide novel approximate analytical expressions for the achievable sum rate, SER, and outage probability along with a detailed high and low-SNR analysis for the achievable sum rate. Section 5 elaborates asymptotic performance on the achievable sum rate of large-system limit at high SNR. The numerical results and the corresponding analysis are presented in Section 6. Section 7 concludes the paper and summarizes the key findings.

As this paper contains many notations, to avoid ambiguity, the reader is referred to Table I for a list of the most frequently used notations.

II. 3D MIMO SYSTEM MODEL

A. D-MIMO FADING MODEL

As in [2], we consider a typical uplink D-MIMO system as illustrated in Fig. 1, where there are one BS with N_r receive

TABLE 1. Main notations definitions.

Notation	Meaning
\mathbb{C}	The set of complex
\mathbb{Z}	The set of real
$\mathbb{E}[\cdot]$	The operation of expectation
$(\cdot)^T$	The transpose operator of a matrix
$(\cdot)^\dagger$	The pseudoinverse operator of a matrix
$(\cdot)^H$	The pseudoinverse operator of a matrix
$(\cdot)^{-1}$	The inverse operator of a matrix
\mathbf{I}_n	The $n \times n$ identity matrix
\oplus	The direct sum operator of matrices
$\text{diag}\{\cdot\}$	The diagonal matrix
$[\mathbf{A}]_{mn}$	The mn th element of matrix \mathbf{A}
$(\cdot)!$	The factorial of a non-negative integer number
$\Gamma(\cdot)$	Gamma function
$\mathcal{G}(m, n)$	Gamma distribution with shape parameter m and scale parameter n
$\mathcal{GG}(\alpha_1, \alpha_2, \beta)$	Generalized Gamma distribution with parameters $\alpha_1, \alpha_2, \beta$
$\mathcal{CW}(m, n)$	Complex Wishart distribution with m degrees of freedom and covariance n
$K_\nu(\cdot)$	Modified Bessel function of the second kind and order ν
$G_{pq}^{mn}[\cdot]$	Meijer's G function with m, n, p, q being non-negative integers
${}_pF_q(\cdot)$	Hypergeometric function for non-negative integers p and q
$\text{Ei}(\cdot)$	Exponential integral function
$\Gamma(a, x) = \int_x^\infty t^{a-1} \exp(-t) dt$	Complementary Gamma function
$Q(\cdot)$	Gaussian Q-function
$\gamma(\alpha, x) = \int_0^x t^{\alpha-1} \exp(-t) dt$	Lower incomplete Gamma function
N_r	The number of BS antennas
L	The number of RAPs
N_t	The number of antennas of each RAP
ρ_l	The correlation coefficient of the RAP antennas
s_l	The shape parameter of Gamma distribution
Ω_l	The scale parameter of Gamma distribution
α_l, β_l	The modulation-specific constants

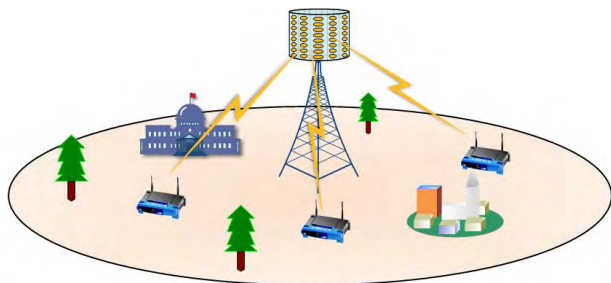


FIGURE 1. Schematic illustration of a D-MIMO system.

antennas and L RAPs each connected to N_t transmit antennas ($N_r \geq LN_t$). Throughout this paper, the following assumptions are adopted: 1) The channel is block fading channel, which means that it remains constant over the block time T and varies independently and identically from one block to another. 2) It is assumed that the BS has perfect channel state information (CSI), while all RAPs have no CSI. Thus, the optimum transmission strategy is to transmit independent and equal power signals from each of the LN_t transmit antennas. Then the corresponding input-output relationship is

$$\mathbf{y} = \sqrt{\frac{P}{LN_t}} \mathbf{H} \mathbf{x} + \mathbf{n} \quad (1)$$

where $\mathbf{y} \in \mathbb{C}^{N_r \times 1}$ denotes the receive signal vector at the BS, $\mathbf{x} \in \mathbb{C}^{LN_t \times 1}$ represents the transmit signal vector from the L RAPs, P is the total transmit power, $\mathbf{n} \in \mathbb{C}^{N_r \times 1}$ is the additive

white Gaussian noise (AWGN) with covariance $\mathbb{E}[\mathbf{nn}^H] = N_0 \mathbf{I}_{N_r}$, where N_0 is the noise power.

The diagonal matrix $\mathbf{\Xi} \in \mathbb{C}^{LN_t \times LN_t}$ captures the large-scale fading, whose elements are independent and identically distributed (i.i.d.) random variables (RVs), which can be expressed as

$$\mathbf{\Xi} = \bigoplus_{l=1}^L \{\mathbf{I}_{N_t} \xi_l / D_l^\nu\} \quad (2)$$

Where D_l is the distance between the BS and the l th RAP, $l = 1, \dots, L$, while ν is the path loss exponent, which is a key parameter to characterize the rate of decay of the signal power with distance, taking values in the range of 2 (corresponding to signal propagation in free space) to 6 [6]. Typical values for the path loss are 4 for an urban macro cell environment and 3 for urban micro cell environment. The coefficient ξ_l captures large-scale shadowing fading, which follows Gamma distribution as

$$p_{\xi_l}(\xi_l) = \frac{\xi_l^{s_l-1}}{\Gamma(s_l) \Omega_l^{s_l}} \exp\left(-\frac{\xi_l}{\Omega_l}\right), \quad \xi_l, \Omega_l, s_l \geq 0 \quad (3)$$

where s_l and $\Omega_l = \mathbb{E}[\xi_l] / s_l$ are the shape and scale parameters of Gamma distribution, respectively, while $\Gamma(\cdot)$ is the Gamma function as defined in [21, eq. (8.310.1)].

The random matrix $\mathbf{H} \in \mathbb{C}^{N_r \times LN_t}$ models the small-scale fading, which is assumed to follow a semi-correlated Rayleigh distribution. The expression can be written as

$$\mathbf{H} = \mathbf{H}_\omega \mathbf{R}_T^{1/2} \quad (4)$$

where the elements of matrix \mathbf{H}_ω are modeled as i.i.d. $\mathcal{CN}(0, 1)$ RVs, while $\mathbf{R}_T \in \mathbb{R}^{LN_t \times LN_t}$ is the transmit correlation matrix which can be expressed as

$$\mathbf{R}_T = \text{diag} \{ \mathbf{R}_{Tl} \}_{l=1}^L \quad (5)$$

where \mathbf{R}_{Tl} denotes the correlation matrix between the transmit antennas of the l th RAP for $l = 1, \dots, L$. It is assumed that the common exponential correlation model is adopted as [22]

$$[\mathbf{R}_{Tl}]_{mn} = \rho_l^{|m-n|}, \quad m, n = 1, \dots, N_t \quad (6)$$

where $\rho_l \in [0, 1]$ is the transmit correlation coefficient. It is noted that transmit correlation only occurs between antennas of the same RAP since different RAPs are, in general, geographically separated.

B. PERFORMANCE WITH ZF RECEIVERS

In the following, we provide the exact analytical expressions on the achievable sum rate, SER, and outage probability of D-MIMO system with ZF receivers over semi-correlated \mathcal{K} fading channels. For convenience of derivation, we define $\mathbf{Z} = \mathbf{H}\mathbf{\Xi}^{1/2}$, and the ZF detector is defined as

$$\mathbf{T}^\dagger = \left(\frac{P}{LN_t} \right)^{-1/2} (\mathbf{Z}^H \mathbf{Z})^{-1} \mathbf{Z}^H \quad (7)$$

After ZF detection, the instantaneous received SNR at the l th output is given as

$$\gamma_l = \frac{\gamma}{LN_t [(\mathbf{Z}^H \mathbf{Z})^{-1}]_{ll}} = \frac{\gamma [\mathbf{\Xi}]_{ll}}{LN_t [(\mathbf{H}^H \mathbf{H})^{-1}]_{ll}} = \xi_l \zeta_l \quad (8)$$

where γ is the average SNR ($\gamma = P/N_0$). The RV ξ_l represents large scale fading coefficient, which follows Gamma distribution $\xi_l \sim \mathcal{G}(s_l, \Omega_l)$ and its PDF is given in (3). For convenience of exposition, we define the RV ζ_l as

$$\zeta_l = \frac{1}{[(\mathbf{H}^H \mathbf{H})^{-1}]_{ll}} \quad (9)$$

where ζ_l denotes small scale fading coefficient, which follows a complex semi-correlated central Wishart distribution $\zeta_l \sim \mathcal{CW}(N_r - LN_t + 1, 1/[\mathbf{R}_T^{-1}]_{ll})$ and its PDF is given as

$$f_{\zeta_l}(\zeta_l) = \frac{\rho_l e^{-\zeta_l \rho_l}}{(N_r - LN_t)!} (\zeta_l \rho_l)^{N_r - LN_t} \quad (10)$$

where ρ_l denotes the l th diagonal element of \mathbf{R}_T^{-1} , while $(\cdot)!$ is the factorial of a non-negative integer number.

Combining (3), (8) with (10), the composite PDF is given as

$$f_{\gamma_l}(\gamma_l) = \frac{2}{(N_r - LN_t)! \Gamma(s_l)} \left(\frac{LN_t D_l^v \rho_l}{\gamma \Omega_l} \right)^{\frac{N_r - LN_t + s_l + 1}{2}} \times \gamma_l^{\frac{N_r - LN_t + s_l - 1}{2}} K_{N_r - LN_t - s_l + 1} \left(2 \sqrt{\frac{LN_t D_l^v \rho_l}{\gamma \Omega_l}} \gamma_l \right) \quad (11)$$

where $K_\nu(\cdot)$ is the modified Bessel function of the second kind and order ν [21, eq. (8.407.1)].

Utilizing a similar line of reasoning as in [3] and [13], the achievable sum rate of D-MIMO system with ZF receivers over semi-correlated \mathcal{K} fading channels can be obtained as

For $\{s_l, N_r - LN_t + 1, N_r - LN_t - s_l + 1\} \in \mathbb{Z}$

$$R = \frac{1}{\ln 2} \frac{1}{(N_r - LN_t)!} \sum_{l=1}^{LN_t} \frac{1}{\Gamma(s_l)} \times G_{42}^{14} \left(\frac{\gamma \Omega_l}{LN_t D_l^v \rho_l} \middle| \begin{matrix} 1 - s_l, LN_t - N_r, 1, 1 \\ 1, 0 \end{matrix} \right) \quad (12)$$

where $G_{pq}^{mn}[\cdot]$ is the Meijer's G function, with m, n, p, q being non-negative integers [21, eq. (9.301)].

For $\{s_l, N_r - LN_t + 1, N_r - LN_t - s_l + 1\} \notin \mathbb{Z}$

$$R = \frac{1}{\ln 2} \sum_{l=1}^{LN_t} \left[\frac{\Gamma(1 - s_l) \Gamma(I - s_l)}{s_l \Gamma(I)} \left(\frac{\rho_l LN_t D_l^v}{\Omega_l \gamma} \right)^{s_l} \times {}_1F_2 \left(s_l; 1 + s_l, s_l - I + 1; -\frac{\rho_l LN_t D_l^v}{\Omega_l \gamma} \right) + \frac{\Gamma(LN_t - N_r) \Gamma(s_l - I)}{(I) \Gamma(s_l)} \left(\frac{\rho_l LN_t D_l^v}{\Omega_l \gamma} \right)^{I-1} \times {}_1F_2 \left(I; I + 1, I + 1 - s_l; -\frac{\rho_l LN_t D_l^v}{\Omega_l \gamma} \right) + \varphi(s_l) + \varphi(I) - \ln \left(\frac{\rho_l LN_t D_l^v}{\Omega_l \gamma} \right) + \frac{\rho_l LN_t D_l^v}{\Omega_l \gamma (s_l - 1) (I - 1)} \times {}_2F_3 \left(1, 1; 2, 2 - s_l, 2 - I; -\frac{\rho_l LN_t D_l^v}{\Omega_l \gamma} \right) \right] \quad (13)$$

where $I = N_r - LN_t + 1$, ${}_pF_q(\cdot)$ is the hypergeometric function for non-negative integer p and q [21, eq. (9.14.1)].

Similarly, the SER of the l -th subchannel of the D-MIMO system with ZF receivers over semi-correlated \mathcal{K} fading channels can be written as [13]

For $\{s_l, N_r - LN_t + 1, N_r - LN_t - s_l + 1\} \in \mathbb{Z}$

$$\text{SER}_l = \frac{\alpha_l}{2\sqrt{\pi} (N_r - LN_t)! \Gamma(s_l)} \times G_{32}^{22} \left(\frac{\gamma \Omega_l \beta_l}{LN_t D_l^v \rho_l} \middle| \begin{matrix} LN_t - N_r, 1 - s_l, 1 \\ 0, 1/2 \end{matrix} \right) \quad (14)$$

For $\{s_l, N_r - LN_t + 1, N_r - LN_t - s_l + 1\} \notin \mathbb{Z}$

$$\text{SER}_l = \frac{\sqrt{\pi} \alpha_l}{(I - 1)! \Gamma(s_l) \sin(\pi(I - s_l))} \times \left[\sum_{m=0}^{\infty} \frac{\left(\frac{LN_t D_l^v \rho_l}{\gamma \Omega_l} \right)^{m+s_l} \Gamma(m+s_l) \Gamma(m+s_l + \frac{1}{2})}{m! \Gamma(m - I + 1 + s_l) 2\beta_l^{m+s_l} \Gamma(m+s_l+1)} - \sum_{m=0}^{\infty} \frac{\left(\frac{LN_t D_l^v \rho_l}{\gamma \Omega_l} \right)^{m+I} \Gamma(m+I) \Gamma(m+I + \frac{1}{2})}{m! \Gamma(m + I + 1 - s_l) 2\beta_l^{m+N_r - LN_t + 1} \Gamma(m+I+1)} \right] \quad (15)$$

where α_l and β_l are modulation-specific constants, typical values for modulation are 1,1 for BPSK and 2, $\sin^2(\pi/M)$ for M-ary PSK [23].

Moreover, the outage probability of the the l -th sub-channel of the D-MIMO system with ZF receivers over semi-correlated \mathcal{K} fading channels can be written as [13]

$$\text{For } \{s_l, N_r - LN_t + 1, N_r - LN_t - s_l + 1\} \in \mathbb{Z}$$

$$P_{out,l}(\gamma_{th}) = \frac{1}{(N_r - LN_t)! \Gamma(s_l)} \times G_{13}^{21} \left(\frac{LN_t D_l^v \rho_l}{\gamma \Omega_l} \gamma_{th} \middle| N_r - LN_t + 1, s_l, 0 \right) \quad (16)$$

$$\text{For } \{s_l, N_r - LN_t + 1, N_r - LN_t - s_l + 1\} \notin \mathbb{Z}$$

$$P_{out,l} = \frac{\pi \csc(\pi(I - s_l))}{(I - 1)! \Gamma(s_l)} \times \frac{{}_1F_2 \left(s_l; 1 + s_l, s_l - I + 1, \frac{\rho_l LN_t D_l^v}{\Omega_l \gamma} \gamma_{th} \right)}{s_l \Gamma(s_l - I + 1) \left(\frac{\rho_l LN_t D_l^v}{\Omega_l \gamma} \gamma_{th} \right)^{s_l}} - \left(\frac{\rho_l LN_t D_l^v}{\Omega_l \gamma} \gamma_{th} \right)^I \times \frac{{}_1F_2 \left(I; I + 1, I - s_l + 1, \frac{\rho_l LN_t D_l^v}{\Omega_l \gamma} \gamma_{th} \right)}{(I) \Gamma(I - s_l)} \quad (17)$$

where γ_{th} is the SNR threshold value.

From the aforementioned analysis, it can be observed that the expressions above involve complicated functions such as Bessel, Meijer's G, and hypergeometric functions, which hinder us to further analyze the performance of the D-MIMO system over semi-correlated \mathcal{K} fading channels and do not provide engineering insights into the impact of system and fading parameters on D-MIMO performance. To overcome this disadvantage, we pursue a tractable approximate analysis by using the moment matching method.

III. EFFICIENT APPROXIMATION

In this section, we devote to using a PDF to approximate the PDF in (11) through the moment matching method. Herein we consider using the Gamma distribution on account of the following reasons:

(1) The PDF of Gamma distribution is simple and tractable, which allows the use of the closed-form expressions developed in [9] and [15] to approximate shadow and composite fading channels.

(2) The Gamma distributions ($\mathcal{G}(\alpha, \beta)$) is a special case of generalized Gamma ($\mathcal{GG}(\alpha_1, \alpha_2, \beta)$) distribution with $\alpha_1 = \alpha$ and $\alpha_2 = 1$, which has been use to approximate Gamma-Gamma distribution [24], [25].¹

For convenience of manipulation, we only match the small-scale and shadowing fading. Then, we define $z_l = \xi_l \zeta_l$. Capitalizing on the result of (11), the PDF of RV z_l can be

¹Generalized Gamma distribution is also known as α - μ distribution. Beside, \mathcal{K} distribution is a special case of Gamma-Gamma distribution with $\alpha = 1$.

evaluated as

$$p_{z_l}(z_l) = \frac{2}{(N_r - LN_t)! \Gamma(s_l)} \left(\frac{\rho_l}{\Omega_l} \right)^{\frac{N_r - LN_t + s_l + 1}{2}} \times z_l^{\frac{N_r - LN_t + s_l - 1}{2}} K_{N_r - LN_t - s_l + 1} \left(2 \sqrt{\frac{\rho_l}{\Omega_l}} z_l \right) \quad (18)$$

Based on (18) and the definition of expectation, the n -th moment of z_l can be expressed as

$$\mathbb{E}[z_l^n] = \frac{\Gamma(N_r - LN_t + 1 + n) \Gamma(s_l + n)}{(N_r - LN_t)! \Gamma(s_l)} \left(\frac{\Omega_l}{\rho_l} \right)^n \quad (19)$$

We define $\chi_l \sim \mathcal{G}(\omega_l, \eta_l)$ as a Gamma RV with a shape parameter ω_l and a scale parameter η_l . Thus, the PDF of χ_l can be derived as [26]

$$p_{\chi_l}(\chi_l) = \frac{\eta_l^{-\omega_l} \chi_l^{\omega_l - 1}}{\Gamma(\omega_l)} \exp\left(-\frac{\chi_l}{\eta_l}\right) \quad (20)$$

Furthermore, the n -th moment of the Gamma RV χ_l can be expressed as [26]

$$\mathbb{E}[\chi_l^n] = \frac{\Gamma(\omega_l + n)}{\Gamma(\omega_l)} \eta_l^n \quad (21)$$

Combining (19) with (21), the relationships between parameters of the approximate PDF and the composite PDF can be derived by matching the first (mean) and second (variance) moments of the two RVs γ_l and χ_l as

$$\omega_l \eta_l = \frac{(N_r - LN_t + 1) s_l \Omega_l}{\rho_l} \quad (22)$$

$$(\omega_l + 1) \omega_l \eta_l^2 = \frac{(I + 1) I (s_l + 1) s_l \Omega_l^2}{\rho_l^2} \quad (23)$$

Solving equations of (22) and (23) with respect to ω_l and η_l , we can obtain the solutions as

$$\omega_l = \frac{(N_r - LN_t + 1) s_l}{N_r - LN_t + s_l + 2} = \frac{1}{A_l} \quad (24)$$

$$\eta_l = \frac{\Omega_l (I + s_l + 1)}{\rho_l} = \frac{\Omega_l I s_l A_l}{\rho_l} \quad (25)$$

$$A_l = \frac{1}{N_r - LN_t + 1} + \frac{1}{s_l} + \frac{1}{(N_r - LN_t + 1) s_l} \quad (26)$$

where A_l is the amount of fading in wireless fading environment as defined in [6], which is used to measure the severity of composite fading channel.

Therefore, the PDF of the approximate Gamma distribution is re-expressed as

$$p_{\chi_l}(\chi_l) = \frac{\left(\frac{\Omega_l (N_r - LN_t + 1) s_l A_l}{\rho_l} \right)^{-\frac{1}{A_l}} \chi_l^{\frac{1}{A_l} - 1}}{\Gamma(1/A_l)} \times \exp\left(-\frac{\chi_l}{\frac{\Omega_l (N_r - LN_t + 1) s_l A_l}{\rho_l}}\right) \quad (27)$$

As the previous analysis, we use a Gamma distribution to approach the composite distribution. Capitalizing on the above approximate PDF, we deduce the closed-form expressions of the achievable sum rate, SER, and outage probability of D-MIMO system with ZF receivers over semi-correlated \mathcal{K} fading channels in section 4, respectively.

IV. APPROXIMATE PERFORMANCE ANALYSIS

In this section, we perform approximate performance analysis of D-MIMO system with ZF receivers by using the derived PDF. To further analyze the effects of the fading parameters on the D-MIMO system, we execute the achievable sum rate analysis in the asymptotically high-SNR and low-SNR regimes. In order to simplify the following manipulations, we use ω_l and η_l to derive the performance, which are determined by (24) and (25).

A. APPROXIMATE ACHIEVABLE SUM RATE ANALYSIS

Motivated by the above discussion, we first derive an approximate achievable sum rate of D-MIMO system with ZF receivers over semi-correlated fading channels, which is proposed in the following theorem.

Theorem 1: The approximate achievable sum rate of D-MIMO system with ZF receivers over semi-correlated \mathcal{K} fading channels is given as

For $\omega_l \in \mathbb{Z}$, we obtain the expression of (28) as

$$R_A = \frac{1}{\ln 2} \sum_{l=1}^{L N_t} \sum_{\mu=0}^{\omega_l-1} \frac{1}{\Gamma(\omega_l - \mu)} \left(-\frac{L N_t D_l^v}{\eta_l p_u} \right)^{\omega_l - \mu - 1} \times \left[-\exp\left(\frac{L N_t D_l^v}{\eta_l p_u}\right) \text{Ei}\left(-\frac{L N_t D_l^v}{\eta_l p_u}\right) + \sum_{k=1}^{\omega_l - \mu - 1} \Gamma(k) \left(-\frac{\eta_l p_u}{L N_t D_l^v} \right)^k \right] \quad (28)$$

where $\text{Ei}(\cdot)$ is the exponential integral function as defined in [21, eq. (8.211.1)].

For $\omega_l \notin \mathbb{Z}$, we obtain the expression of (29) as

$$R_A = \frac{1}{\ln 2} \sum_{l=1}^{L N_t} \left\{ \left(\frac{L N_t D_l^v}{\eta_l \gamma} \right)^{\omega_l} \pi \Gamma(1 - \omega_l) \times G_{31}^{11} \left[\frac{\eta_l \gamma}{L N_t D_l^v} \middle| \begin{matrix} 1, \omega_l + 1, 1/2 \\ \omega_l, 1/2 \end{matrix} \right] + \ln \left(\frac{\eta_l \gamma}{L N_t D_l^v} \right) + \varphi(\omega_l) + \frac{\pi L N_t D_l^v \Gamma(2 - \omega_l)}{\eta_l \gamma (1 - \omega_l)} G_{32}^{21} \left[-\frac{\eta_l \gamma}{L N_t D_l^v} \middle| \begin{matrix} 1, 2, 2 - \omega_l \\ 1, 1 \end{matrix} \right] \right\} \quad (29)$$

Proof: A detail proof is provided in Appendix I. \square

Corollary 1: For i.i.d \mathcal{K} fading channels ($L = 1, \Omega = 1, \rho = 1$), the approximate achievable sum rate reduces to

$$R_A = \frac{N_t}{\ln 2} \exp\left(\frac{N_t D^v}{\eta \gamma}\right) \sum_{k=1}^{\omega} \left(\frac{\eta \gamma}{N_t D^v} \right)^{k-\omega} \times \Gamma\left(k - \omega, \frac{N_t D^v}{\eta \gamma}\right) \quad (30)$$

where $\Gamma(a, x) = \int_x^\infty t^{a-1} \exp(-t) dt$ is the complementary Gamma function as defined in [21, eq.(8.350.2)].

Proof: The proof starts by utilizing the theorem 1 and taking $L = 1, \Omega = 1, \rho = 1$, then we apply the expressions of [6, eq.(15.24)] and [6, eq.(15.B7)]. After some simple manipulations, we can conclude the proof. \square

Note that the derived expressions of the sum rate in theorem 1 and corollary 1 can be simplified, especially for the case of ω_l setting as integers. For $\omega_l \in \mathbb{Z}$, the final analytical expressions involve simple functions, which can be more efficiently evaluated and provide practical insights for systems design. However, they do not offer useful insights into the effects of system parameters such as fading parameters and the number of antennas. To this end, the high and low SNR asymptotic analyses are considered, respectively.

Corollary 2: For high-SNRs, the approximate sum rate of D-MIMO system with ZF receivers over semi-correlated \mathcal{K} Fading channels is given by

$$R_A^H = L N_t \log_2 \left(\frac{\gamma}{L N_t} \right) + \sum_{l=1}^{L N_t} \left[\frac{1}{\ln 2} \varphi \left(\frac{I_{s_l}}{I + s_l + 1} \right) + \log_2 \left(\frac{\Omega_l (I + s_l + 1)}{\rho_l} \right) - \log_2 (D_l^v) \right] \quad (31)$$

Proof: The proof starts by taking γ large in (43) and applying the integral identity [21, eq.(4.352.1)]

$$\int_0^\infty x^{v-1} \exp(-\mu x) \ln x dx = \frac{\Gamma(v)}{\mu^v} [\varphi(v) - \ln(\mu)], \quad \text{Re}(\mu, v) > 0 \quad (32)$$

and after some manipulations, we can complete the proof. \square

The result in (31) reveals that the proposed approximate sum rate increases logarithmically with the transmit power and the number of receiver antennas when the SNR is large, which is consistent with the result of [3]. Furthermore, we can also observe that the proposed approximate sum rate also decreases with the transceiver distances. Similar results appear in [18].

In general, the low-SNR performance analysis of any MIMO channels can be investigated by taking the first order expansion of the sum rate around $p_u = \gamma = 0^+$. Nevertheless, this approach is vulnerable because it does not reflect the impact of the channel and leads to misleading results in the low-SNR regime. Thus, we explore the low-SNR sum rate via the normalized transmit energy per bit E_b/N_0 rather than per-SNR, which is originally proposed in [27]. The approximate sum rate in the low-SNR regime can be expressed as

$$R_A^L \left(\frac{E_b}{N_0} \right) \approx S_0 \log_2 \left(\frac{\frac{E_b}{N_0}}{\frac{E_b}{N_{0 \min}}} \right) \quad (33)$$

$$\frac{E_b}{N_{0 \min}} = \frac{1}{\dot{R}_A(0)}, \quad S_0 = -2 \ln 2 \frac{(\ddot{R}_A(0))^2}{\dot{R}_A(0)} \quad (34)$$

where $\frac{E_b}{N_{0 \min}}$ and S_0 are the two key parameters for the low-SNR analysis, which represent minimum normalized energy per information bit to reliably convey any positive rate and wideband slope, respectively. $\dot{R}_A(0)$ and $\ddot{R}_A(0)$ are the first and second derivatives of the approximate sum rate in (46)

with respect to SNR γ . We then investigate the low-SNR regime in the following proposition.

Proposition 1: The minimum energy per information bit and wideband of D-MIMO system with ZF receivers over semi-correlated \mathcal{K} fading channels are derived, respectively

$$\frac{E_b}{N_{0 \min}} = \frac{LN_t}{\log_2(e)} \left(\sum_{l=1}^{LN_t} \frac{\omega_l \eta_l}{D_l^v} \right)^{-1} \quad (35)$$

$$S_0 = \frac{2N_t \left(\sum_{l=1}^{LN_t} \frac{\omega_l \eta_l}{D_l^v} \right)^2}{\sum_{l=1}^{LN_t} \frac{\omega_l(\omega_l+1)\eta_l^2}{D_l^{2v}}} \quad (36)$$

Proof: The proof is provided in Appendix II. \square

Clearly, the required minimum energy per bit increases with the distances between BS and RAPs while decreases with the parameters ω_l and η_l . We also note that the wideband slope in (36) is greater than one based on the binomial expansion formula.

B. APPROXIMATE SER ANALYSIS

We then analyze the approximate SER of D-MIMO system with ZF receivers over semi-correlated \mathcal{K} fading channels. Based on the generic formula of [23], the approximate SER of modulation formats (e.g. BPSK, M-ary PSK, M-ary PAM) can be given as

$$\text{SER}_{A,l} \triangleq \alpha_l \mathbb{E} \left[Q \left(\sqrt{2\beta_l \gamma_l} \right) \right], \quad l = 1, \dots, LN_t \quad (37)$$

where $Q(\cdot)$ is the Gaussian Q-function as defined in [6], while α_l and β_l represent the modulation-specific constants, which are key parameters to characterize modulation model. The values are $\alpha_l = 1, \beta_l = 1$ for BPSK while $\alpha_l = 2$ and $\beta_l = \sin(\pi/M)$ for M-ary PSK [23]. The approximate analytical expression for the l -th SER is given in the following theorem.

Theorem 2: The approximate SER of the l -th subchannel of D-MIMO system with ZF receivers over semi-correlated \mathcal{K} fading channels is provided as

For $\omega_l \in \mathbb{Z}$, the approximate SER is given by (38)

$$\text{SER}_{A,l} = \frac{\alpha_l}{2} \left[1 - \mu(c) \sum_{k=0}^{\omega_l-1} \binom{2k}{k} \left(\frac{1 - [\mu(c)^2]}{4} \right)^k \right] \quad (38)$$

For $\omega_l \notin \mathbb{Z}$, the approximate SER is given by (39)

$$\text{SER}_{A,l} = \frac{\alpha_l \sqrt{c}}{2(1+c)^{\omega_l+\frac{1}{2}}} G_{33}^{21} \left[1+c \left| \begin{matrix} 1, \frac{1}{(1+c)}, \frac{1}{2} \\ 1, \omega_l + \frac{1}{2}, \frac{1}{2} \end{matrix} \right. \right] \quad (39)$$

where $c = \frac{\gamma \eta_l \beta_l}{LN_t D_l^v}$, $\mu(c) = \sqrt{\frac{c}{1+c}}$.

Proof: A detailed proof is given in Appendix III.

It is worth noting that the SER decreases with the parameters ω_l and η_l while increases with the modulation-specific

constant α_l . More importantly, the approximate analytical expression of SER for $\{\omega_l\} \in \mathbb{Z}$ only involves the simple functions.

C. APPROXIMATE OUTAGE PROBABILITY ANALYSIS

When considering the case of non-ergodic channels such as quasi-static or block-fading, it is appropriate to investigate the outage probability performance of D-MIMO system with ZF receivers over the approximate PDF. The outage probability, $P_{out,l}$, is defined as the probability that the instantaneous error probability is less than or equal to a specified value that the output SNR falls below a certain specified threshold, γ_{th}

$$P_{out,l} \triangleq \Pr(\gamma_l \leq \gamma_{th}) \quad (40)$$

Based on this definition, we investigate the approximate outage probability performance of D-MIMO system with ZF receivers in the following theorem.

Theorem 3: The outage probability of the l -th subchannel of D-MIMO system with ZF receivers over the approximate PDF is derived as

For $\omega_l \in \mathbb{Z}$, the approximate outage probability is given by (41)

$$P_{out,l} = 1 - \exp\left(-\frac{LN_t D_l^v}{\eta_l \gamma} \gamma_{th}\right) \sum_{k=0}^{\omega_l-1} \frac{\gamma_{th}^k}{k!} \left(\frac{LN_t D_l^v}{\eta_l \gamma}\right)^k \quad (41)$$

For $\omega_l \notin \mathbb{Z}$, the approximate outage probability is given by (42)

$$P_{out,l} = \frac{1}{\Gamma(\omega_l)} \gamma \left(\omega_l, \frac{LN_t D_l^v}{\gamma \eta_l} \right) \quad (42)$$

where $\gamma(\alpha, x) = \int_0^x t^{\alpha-1} \exp(-t) dt$ is the lower incomplete Gamma function as defined in [28].

Proof: The proof is provide in Appendix IV. \square

From theorem 3, we can see that the outage probability is suffered from the effects of the number of RAPs L , the number of antennas of each RAP N_t , transmit power γ , the distances D_l between BS and RAP, and SNR threshold γ_{th} . The outage probability increases with the parameters L, N_t, D_l and γ_{th} , while decreases with γ and η_l .

V. ASYMPTOTIC SUM RATE ANALYSIS

Recently, large-scale MIMO has demonstrated great potential to provide significant capacity and power savings, and has been known as a disruptive technology for the future 5G wireless communication [17], [29]. In the following, we pursue a large-system analysis and provide sum rates by using the result of corollary 2.

(i) Fixed L, N_t, γ , while $N_r \rightarrow \infty$: It is quite intuitive that the received SNR grows into infinity when the number of receive antennas grows without bound whilst keeping L, N_t, γ fixed.

Corollary 3: For D-MIMO composite fading channel, as N_r growing into infinity and L, N_t, γ keeping fixed, the

asymptotic approximate sum rate converges to

$$\bar{R}_A^H \stackrel{N_r \rightarrow \infty}{\approx} LN_t \log_2 \left(\frac{\gamma N_r}{LN_t} \right) + \sum_{l=1}^{LN_t} \left[\frac{\varphi(s_l)}{\ln 2} + \log_2 \left(\frac{\Omega_l}{\rho_l} \right) - \log_2(D_l^v) \right] \quad (43)$$

Proof: The proof starts by taking $N_r \rightarrow \infty$ of (31). After some approximate manipulations, we complete the proof of corollary 3. \square

From corollary 3, we can conclude that the effects of small-scale fading are eliminated with $N_r \rightarrow \infty$ and fixed L, N_t, γ . The similar result can be found in [18]. Moreover, we can also observe that the asymptotic sum rate increase logarithmically with γ and N_r , while decreases with D_l .

(ii) Fixed L, N_t, E_u , and $N_r \rightarrow \infty$, let $\gamma = E_u/N_r$: In this scenario, we can scale down transmit power to γ/N_r with no reduction in performance. This is relevant in practice since it is vital not only from a business point of view but also to address environment and health concerns.

Corollary 4: For D-MIMO composite fading channels, as N_r grows into infinity with fixed L, N_t, E_u , the asymptotic approximate sum rate approaches

$$\bar{R}_A^H \stackrel{N_r \rightarrow \infty}{\approx} LN_t \log_2 \left(\frac{E_u}{LN_t} \right) + \sum_{l=1}^{LN_t} \left[\frac{\varphi(s_l)}{\ln 2} + \log_2 \left(\frac{\Omega_l}{\rho_l} \right) - \log_2(D_l^v) \right] \quad (44)$$

Proof: Starting by taking $N_r \rightarrow \infty$ of (31) and $\gamma = E_u/N_r$, we can conclude the proof after some approximate manipulations. \square

Through corollary 4, we can observe that as the number of receiver antennas grows to infinity, the transmit power of each RAP can be cut proportionally to $1/N_r$ without loss of performance. The same result is proposed in [18] and [19]. Besides, we can find that the asymptotic approximate sum rate tends to a deterministic constant when the number of the receive antenna grows into infinity.

(iii) Fixed L, N_t, γ, κ , and $N_r, L \rightarrow \infty$, letting $\kappa = N_r/LN_t$: This asymptotic scenario is significant in theory and practice since N_r is large but not much greater than LN_t . Note that this scenario consists two separate cases: i) fixed N_t while $L \rightarrow \infty$ and ii) fixed L while $N_t \rightarrow \infty$. The two cases receive similar results. Therefore, we only take the case i) into account.

Corollary 5: For D-MIMO composite fading channel, when the numbers of N_r and L grow into infinity with a fixed ratio $N_r/(LN_t) \geq 1$, the asymptotic approximate sum rate tends to

$$\bar{R}_A^H \stackrel{N_r, L \rightarrow \infty}{\approx} LN_t \log_2 (\gamma (\kappa - 1)) + \sum_{l=1}^{LN_t} \left[\frac{\varphi(s_l)}{\ln 2} + \log_2 \left(\frac{\Omega_l}{\rho_l} \right) - \log_2(D_l^v) \right] \quad (45)$$

Proof: The proof starts by taking $N_r, L \rightarrow \infty$ of (31) and substituting $\kappa = N_r/LN_t$ into (31), then we can obtain (45)

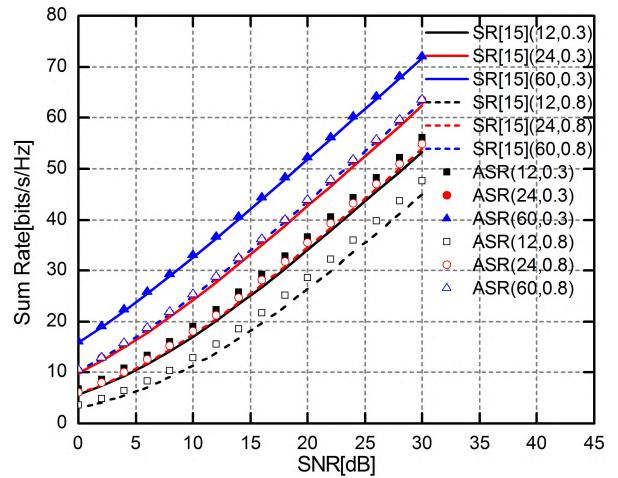


FIGURE 2. Sum rate and approximate sum rate versus SNR ($N_r = 12, 24, 60, N_t = 2, L = 3, \rho_l = 0.3, 0.8, s_l = 1, \Omega_l = 1, v = 4, D_1 = 1000m, D_2 = 1500m, D_3 = 2000m$, the tuple in the legend represents (N_r, ρ) , SR and ASR represent sum rate and approximate, respectively).

after appropriate simplifications. We can conclude the proof of corollary 5. \square

The result of corollary 5 reveals that the asymptotic approximate result increases linearly with the number of RAPs and logarithmically with transmit power γ and κ . This result is identical with the result of [19].

From corollary 3, 4, and 5, we can conclude some common characteristic: First, the effect of small-scale fading can be canceled for large number of receive antennas. Second, the proposed sum rate increases with the numbers of transceiver antennas and the transmit power while decreases with the transceiver distances.

VI. NUMERICAL RESULTS

In this section, some numerical results are provided to validate the accuracy of our analysis in section 4 and section 5. Through this section, it is assumed that there are $L = 3, N_t = 2$ in all simulated settings.

In Fig. 2, we compare the proposed approximate sum rate of (28) with the analytical sum rate of [13, eq. (13)] for different transmit correlation coefficient $\rho_l = 0.3, 0.8$. In this simulation, we set $N_r = 12, 24, 60, N_t = 2, L = 3, \rho_l = 0.3, 0.8, s_l = 1, \Omega_l = 1, v = 4, D_1 = 1000m, D_2 = 1500m, D_3 = 2000m, l = 1, \dots, L$. It can be readily observed from Fig. 2 that the proposed approximate sum rate is sufficiently tight across the entire SNR range of interest for different value of ρ_l , especially when the number of receive antenna is $N_r = 60$, thereby validating the correctness of the proposed approximate expressions. The figure shows that adding more receive antennas significantly stabilizes the MIMO link by improving the receive diversity and reducing the noise enhancement effect. Further, for large N_r , the proposed approximate sum rate becomes almost exact with the analytical sum rate. In addition, Fig. 2 also indicates that

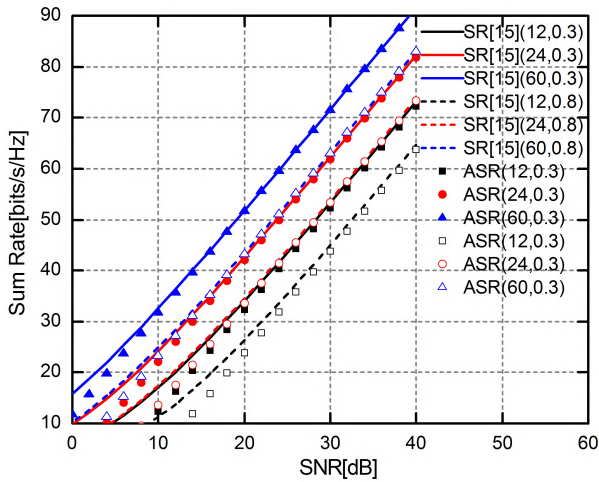


FIGURE 3. Sum rate and approximate sum rate for high SNR ($N_r = 12, 24, 60, N_t = 2, L = 3, \rho_l = 0.3, 0.8, s_l = 1, \Omega_l = 1, v = 4, D_1 = 1000m, D_2 = 1500m, D_3 = 2000m$, the tuple in the legend represents (N_r, ρ) , SR and ASR represent sum rate and approximate sum rate, respectively).

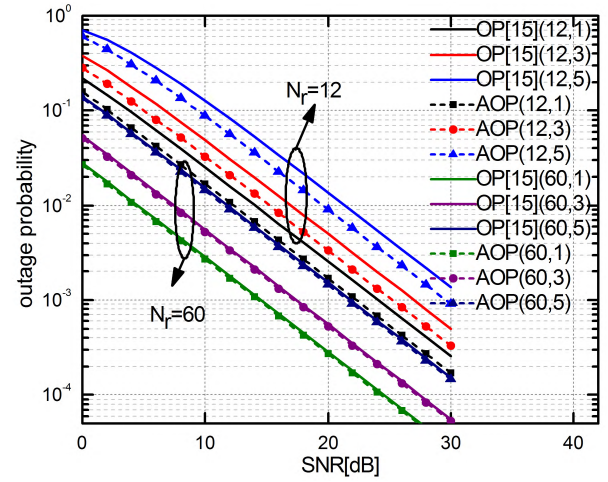


FIGURE 5. Simulated outage probability and approximate outage probability versus SNR ($N_r = 12, 60, N_t = 2, L = 3, \rho_l = 0.5, s_l = 1, \Omega_l = 1, v = 3, D_1 = 800m, D_2 = 1000m, D_3 = 1400m, \gamma_{th} = 1$, the tuple in the legend represents (N_r, l) , OP, AOP and l represent outage probability, approximate outage probability and the l -th subchannel, respectively).

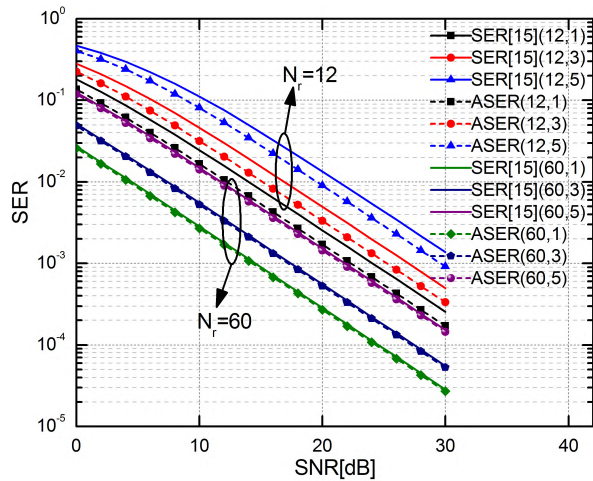


FIGURE 4. Simulated SER and approximate SER versus SNR ($N_r = 12, 60, N_t = 2, L = 3, \rho_l = 0.5, s_l = 1, \Omega_l = 1, v = 3, D_1 = 800m, D_2 = 1000m, D_3 = 1400m, \alpha = 2, \beta = 0.5$, the tuple in the legend represents (N_r, l) , ASER and l represent approximate SER and the l -th subchannel, respectively).

spatial correlation limits the advantages of D-MIMO system due to the reduced diversity.

Comparisons between the approximate sum rate (31) and the analytical sum rate of [13, eq. (16)] at high SNR with different values of ρ are presented in Fig. 3. For the sake of simplicity, the parameter settings are the same as Fig. 2. As anticipated, the match between approximate sum rate and analytical sum rate becomes more excellent for the high SNR and when the number of antennas grows large. At high SNR, the sum rate performance increases linearly with SNR. As similar with Fig 2, the sum rate decreases with the value ρ_l due to the reduced diversity.

Fig. 4 illustrates the impact of SNR on the approximate SER in (38) and the analytical SER in [13, eq. (40)] for

different BS antennas N_r . In this simulation, the parameters are set as follows: $N_r = 12, 60, N_t = 2, L = 3, \rho_l = 0.5, s_l = 1, \Omega_l = 1, v = 3, D_1 = 800m, D_2 = 1000m, D_3 = 1400m$.² In addition, all subchannels are using QPSK modulation with modulation parameters $\alpha = 2, \beta = 0.5$. The figure indicates that the difference between approximate SER and the analytical SER is about 0.8 dB for $N_r = 12$. When $N_r = 60$, the approximate expression in (38) almost coincides with the analytical expression of [13, eq. (40)].

In Fig. 5, the individual subchannel approximate outage probability in (41) and analytical outage probability in [13, eq. (49)] against the SNR for a fixed threshold $\gamma_{th} = 1$ is addressed. It is noted that the settings of parameters in Fig. 5 are the same as that of Fig. 4. From Fig. 5, we can observe that the gap between the proposed approximate expression in (41) and the analytical expression in [13, eq.(49)] decreases as N_r gets large. For instance, when $N_r = 12$, there is about 1.76 dB between the (41) and [13, eq.(49)]. However, when $N_r = 60$, the difference is about 0.11 dB. Thus, there is a sufficient agreement between the proposed approximate expression and the analytical expression for $N_r = 60$. In addition, the 5th subchannel correspond to the pessimistic performance due to the highest transceiver distance and the strongest path loss.

In Fig. 6, we analyze the proposed approximate sum rate versus the number of receive antennas N_r for the case of $P = 30$ dB and $P/N_r = 30$ dB, respectively. For $P = 30$ dB, the approximate sum rate and the analytical sum rate increase logarithmically with the value N_r , and the

²Note that each subchannel of the same RAP experiences the same SER and outage probability since each has the same distance and location, thus we only simulate the performance (SER and outage probability) of L subchannels in section 6.

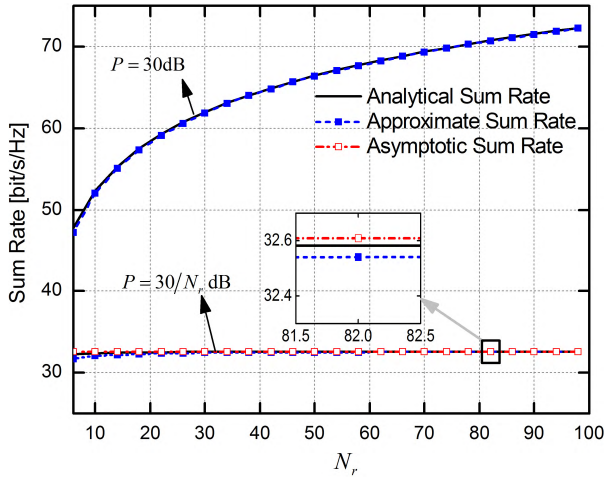


FIGURE 6. Simulated sum rate, approximate sum rate and asymptotic sum rate versus the number of receive antennas ($N_t = 2$, $L = 3$, $\rho_l = 0.5$, $s_l = 1$, $\Omega_l = 1$, $v = 4$, $D_1 = 1000m$, $D_2 = 1500m$, $D_3 = 2000m$).

approximate sum rate is sufficiently tight for arbitrary number of receive antennas N_r . For $P/N_r = 30$, the performances of approximate sum rate and the analytical sum rate converge to a deterministic constant when the number of receive antennas N_r grows into infinity. More importantly, we can observe that the curves of the asymptotic approximate sum rate and the approximate sum rate overlap with the analytical sum rate.

VII. CONCLUSION

In this paper, we investigate the approximate performance of D-MIMO system with ZF receivers over semi-correlated \mathcal{K} fading channels. First, we approximate the composite distribution with a Gamma distribution employing moment matching method. Then, we derive the novel approximate expressions for the achievable sum rate, SER and outage probability of the D-MIMO systems with ZF receivers by using the derived distribution function. In parallel, we present the tractable closed-form approximations in the asymptotically high and low SNR regimes. It is demonstrated that the derived expressions become extremely exact across the entire SNRs for large value N_r . Based on the approximate sum rate, we pursue the large system analysis at high SNR. Through the previous analysis, we can conclude that the approximate Gamma distribution derived by the moment matching method relatively approaches the composite distribution, and the derived expressions provide the engineering insights for practical system design. However, this approximate analysis is only applicable to integer parameters. How to tame the approximate analysis for non-integer parameters is left to the future work.

APPENDIX I PROOF OF THEOREM 1

Proof: The proof starts by using the PDF of RV χ_l to approximate the PDF of RV ζ_l . Thus, the achievable sum rate can be

expressed as

$$R_A = \sum_{l=1}^{LN_t} \mathbb{E} \left[\log_2 \left(1 + \frac{\gamma}{LN_t D_l^v} \chi_l \right) \right] \quad (46)$$

The above expression can be further re-written in integral form as

$$R_A = \frac{1}{\ln 2} \sum_{l=1}^{LN_t} \int_0^\infty \ln \left(1 + \frac{\gamma}{LN_t D_l^v} \chi_l \right) p_{\chi_l}(\chi_l) d\chi_l \quad (47)$$

Substituting (19) into (44), we can obtain

$$R_A = \frac{1}{\ln 2} \sum_{l=1}^{LN_t} \frac{\eta_l^{-\omega_l}}{\Gamma(\omega_l)} \times \int_0^\infty \ln \left(1 + \frac{\gamma}{LN_t D_l^v} \chi_l \right) \chi_l^{\omega_l-1} \exp \left(-\frac{\chi_l}{\eta_l} \right) d\chi_l \quad (48)$$

For $\omega_l \in \mathbb{Z}$, we can obtain the final expression by adopting the result of [30]

$$R_A = \sum_{l=1}^{LN_t} \sum_{\mu=0}^{\zeta_l} \frac{\zeta_l!}{(\zeta_l - \mu)!} \left[\frac{(-1)^{\zeta_l-\mu-1}}{a_l^{\zeta_l-\mu}} \exp \left(-\frac{1}{a_l} \right) \times \text{Ei} \left(-\frac{1}{a_l} \right) + \sum_{k=1}^{\zeta_l-\mu} \Gamma(k) \left(-\frac{1}{a_l} \right)^{\zeta_l-\mu-k} \right] \quad (49)$$

where $a_l = \frac{\gamma}{LN_t D_l^v}$ and $\zeta_l = \omega_l - 1$.

Substituting $a_l = \frac{\gamma}{LN_t D_l^v}$ and $\zeta_l = \omega_l - 1$ into (49), we can obtain the result of (27).

For $\omega_l \notin \mathbb{Z}$, we use the following integral identity as [31, eq. (2.6.23.4)]

$$\int_0^\infty x^{\alpha-1} \exp(-px) \ln(a+bx) dx = \left(\frac{a}{b} \right)^\alpha \frac{\pi}{\alpha \sin(\alpha\pi)} \times {}_1F_1 \left(\alpha; \alpha + 1; \frac{ap}{b} \right) - \Gamma(\alpha) p^{-\alpha} \times \left\{ \ln \left(\frac{p}{b} \right) - \varphi(\alpha) - \frac{ap}{b(1-\alpha)} {}_2F_2 \left(1, 1; 2, 2 - \alpha; \frac{ap}{b} \right) \right\} \quad (50)$$

Substituting (47) into (45), the achievable sum rate of (45) can be further re-expressed

$$R_A = \frac{1}{\ln 2} \sum_{l=1}^{LN_t} \left(\frac{LN_t D_l^v}{\eta_l \gamma} \right)^{\omega_l} \frac{\pi}{\omega_l \sin(\omega_l \pi) \Gamma(\omega_l)} \times {}_1F_1 \left(\omega_l; \omega_l + 1; \frac{LN_t D_l^v}{\eta_l \gamma} \right) - \ln \left(\frac{LN_t D_l^v}{\eta_l \gamma} \right) + \varphi(\omega_l) + \frac{LN_t D_l^v}{\eta_l \gamma (1 - \omega_l)} {}_2F_2 \left(1, 1; 2, 2 - \omega_l; \frac{LN_t D_l^v}{\eta_l \gamma} \right) \quad (51)$$

using the following Euler's reflection formula [32, eq. (2.10.2)]

$$\frac{\pi}{\sin(\pi\omega_l)} = \Gamma(\omega_l) \Gamma(1 - \omega_l) \quad (52)$$

in addition, expressing the hypergeometric functions ${}_1F_1(\cdot)$ and ${}_2F_2(\cdot)$ via Meijer-G function [33, eq. (07.20.26.0005.01)] and [33, eq. (07.25.26.0004.01)]

$${}_1F_1(a; b; z) = \frac{\pi \Gamma(b)}{\Gamma(a)} G_{23}^{11} \left[z \left| \begin{matrix} 1-a, 1/2 \\ 0, 1-b, 1/2 \end{matrix} \right. \right] \quad (53)$$

$$\begin{aligned} {}_2F_2(a_1, a_2; b_1, b_2; z) &= \frac{\pi \Gamma(b_1) \Gamma(b_2)}{\Gamma(a_1) \Gamma(a_2)} \\ &\times G_{23}^{12} \left[-z \left| \begin{matrix} 1-a_1, 1-a_2 \\ 0, 1-b_1, 1-b_2 \end{matrix} \right. \right] \end{aligned} \quad (54)$$

Substituting (52), (53), (54) into (51), formula (51) can be further simplified as

$$\begin{aligned} R_A &= \frac{1}{\ln 2} \sum_{l=1}^{LN_t} \left\{ \left(\frac{LN_t D_l^v}{\eta_l \gamma} \right)^{\omega_l} \pi \Gamma(1 - \omega_l) \right. \\ &\times G_{23}^{11} \left[\frac{LN_t D_l^v}{\eta_l \gamma} \left| \begin{matrix} 1 - \omega_l, \frac{1}{2} \\ 0, -\omega_l, \frac{1}{2} \end{matrix} \right. \right] + \ln \left(\frac{\eta_l \gamma}{LN_t D_l^v} \right) + \varphi(\omega_l) \\ &\left. + \frac{\pi LN_t D_l^v \Gamma(2 - \omega_l)}{\eta_l \gamma (1 - \omega_l)} G_{23}^{12} \left[-\frac{LN_t D_l^v}{\eta_l \gamma} \left| \begin{matrix} 0, 0 \\ 0, -1, \omega_l - 1 \end{matrix} \right. \right] \right\} \end{aligned} \quad (55)$$

Utilizing the following identity [21, eq. (9.31.2)]

$$G_{pq}^{mn} \left[x^{-1} \left| \begin{matrix} \mathbf{a}_r \\ \mathbf{b}_s \end{matrix} \right. \right] = G_{qp}^{nm} \left[x \left| \begin{matrix} 1 - \mathbf{b}_s \\ 1 - \mathbf{a}_r \end{matrix} \right. \right] \quad (56)$$

Substituting (56) into (55), we can obtain the result of (28). Therefore, we complete the proof of Theorem 1.

APPENDIX II PROOF OF PROPOSITION 1

The proof starts by taking the first and second derivatives of (43) with respect to γ . For $\gamma \rightarrow 0$, we can obtain as

$$\begin{aligned} \dot{R}_A(0) &= \frac{1}{\ln 2} \sum_{l=1}^{LN_t} \mathbb{E} \left[\left. \frac{\frac{1}{LN_t D_l^v} \chi_l}{1 + \frac{\gamma}{LN_t D_l^v} \chi_l} \right|_{\gamma=0} \right] \\ &= \frac{\log_2(e)}{LN_t} \sum_{l=1}^{LN_t} \mathbb{E} \left[\frac{\chi_l}{D_l^v} \right] \end{aligned} \quad (57)$$

$$\begin{aligned} \ddot{R}_A(0) &= -\frac{1}{\ln 2} \sum_{l=1}^{LN_t} \mathbb{E} \left[\left. \frac{\left(\frac{1}{LN_t D_l^v} \chi_l \right)^2}{\left(1 + \frac{\gamma}{LN_t D_l^v} \chi_l \right)^2} \right|_{\gamma=0} \right] \\ &= -\frac{\log_2(e)}{(LN_t)^2} \sum_{l=1}^{LN_t} \mathbb{E} \left[\frac{\chi_l^2}{D_l^{2v}} \right] \end{aligned} \quad (58)$$

The above expressions in (53) and (54) can be further simplified by combining the definition of expectation with

the PDF of χ_l in (19)

$$\dot{R}_A(0) = \frac{\log_2(e)}{LN_t} \sum_{l=1}^{LN_t} \frac{\omega_l \eta_l}{D_l^v} \quad (59)$$

$$\ddot{R}_A(0) = -\frac{\log_2(e)}{(LN_t)^2} \sum_{l=1}^{LN_t} \frac{\omega_l (\omega_l + 1) \eta_l^2}{D_l^{2v}} \quad (60)$$

Substituting (55) and (56) into (33), we can derive the result of proposition after simple manipulations. Then we conclude the proof of proposition 1.

APPENDIX III PROOF OF THEOREM 2

Proof: The proof starts from (20), we can obtain the approximate PDF of γ_l as

$$\begin{aligned} p_{\gamma_l}(\gamma_l) &= \frac{LN_t D_l^v}{\gamma} p_{\chi_l} \left(\frac{LN_t D_l^v}{\gamma} \right) \\ &= \frac{1}{\Gamma(\omega_l)} \left(\frac{LN_t D_l^v}{\gamma \eta_l} \right)^{\omega_l} \gamma_l^{\omega_l - 1} \exp \left(-\frac{LN_t D_l^v}{\gamma \eta_l} \gamma_l \right) \end{aligned} \quad (61)$$

Combining (57) with the expression in [6, eq. (4.2)], we can express the SER in (37) in integral form as

$$\begin{aligned} \text{SER}_{A,l} &= \frac{\alpha_l \eta_l^{-\omega_l}}{\pi \Gamma(\omega_l)} \left(\frac{LN_t D_l^v}{\gamma} \right)^{\omega_l} \int_0^{\frac{\pi}{2}} \int_0^{\infty} \gamma_l^{\omega_l - 1} \exp \\ &\times \left[-\left(\frac{\beta_l}{\sin^2(\theta)} + \frac{LN_t D_l^v}{\eta_l \gamma} \right) \gamma_l \right] d\gamma_l d\theta \end{aligned} \quad (62)$$

Applying the integral identity [21, eq. (3.381.4)]

$$\int_0^{\infty} x^{v-1} \exp(-\mu x) dx = \frac{1}{\mu^v} \Gamma(v) \quad (63)$$

the expression in (62) can be further simplified as

$$\text{SER}_{A,l} = \frac{\alpha_l}{\pi} \int_0^{\frac{\pi}{2}} \left(\frac{\beta_l \eta_l \gamma / LN_t D_l^v}{\sin^2(\theta)} + 1 \right)^{-\omega_l} d\theta \quad (64)$$

When $\{\omega_l\} \in \mathbb{Z}$, the expression in (64) can be re-written via the result of [34]

$$\begin{aligned} \text{SER}_{A,l} &= \sqrt{\frac{c}{1+c}} \frac{(1+c)^{-\omega_l} \Gamma(\omega_l + \frac{1}{2}) \Gamma(\omega_l + 1) (1+c)^{\omega_l}}{2\sqrt{\pi} \Gamma(\omega_l + 1) \left(\frac{1}{2}\right)_{\omega_l}} \\ &\times \left[\sqrt{\frac{1+c}{c}} - \sum_{k=0}^{\omega_l - 1} \frac{(1/2)_k}{k!} \left(\frac{1}{1+c}\right)^k \right] \end{aligned} \quad (65)$$

where $(a)_b = \frac{\Gamma(a+k)}{\Gamma(a)} = a(a+1)\dots(a+k-1)$ and $c = \frac{\gamma \eta_l \beta_l}{LN_t D_l^v}$.

Substituting $\sqrt{\pi} \left(\frac{1}{2}\right)_{\omega_l} = \Gamma(\omega_l + 1/2)$ and $\frac{(1/2)_k}{k!} = \binom{2k}{k} \left(\frac{1}{4}\right)^k$ into (65), we can derived the expression as

$$\text{SER}_{A,l} = \frac{1}{2} \left[1 - \sqrt{\frac{c}{1+c}} \sum_{k=0}^{n-1} \binom{2k}{k} \left(\frac{1}{4(1+c)}\right)^k \right] \quad (66)$$

Letting $\mu(c) = \sqrt{\frac{c}{1+c}}$, we can derive the expression of (37).

When $\{\omega_l\} \notin \mathbb{Z}$, the expression in (64) can be simplified by using [34, eq. (A8)]

$$\begin{aligned} \text{SER}_{A,l} &= \sqrt{\frac{c}{c+1}} \frac{(1+c)^{-\omega_l} \Gamma(\omega_l + 1/2)}{2\sqrt{\pi} \Gamma(\omega_l + 1)} \\ &\times {}_1F_1\left(1, \omega_l + \frac{1}{2}; \omega_l + 1; \frac{1}{1+c}\right) \end{aligned} \quad (67)$$

Applying the formula [33, eq. (07.23.26.0005.01)] and (52)

$$\begin{aligned} {}_2F_1(a, b; c; z) &= \frac{\pi \Gamma(c)}{\Gamma(a) \Gamma(b)} \\ &\times G_{33}^{12}\left[z \left| \begin{matrix} 1-a, 1-b, 1/2 \\ 0, 1-c, 1/2 \end{matrix} \right. \right] \end{aligned} \quad (68)$$

After simple simple manipulations, we can obtain the result of (38). Thus, we conclude the proof of the theorem 2.

**APPENDIX IV
PROOF OF THEOREM 3**

Proof: The proof starts by combining the definition of outage probability in (40) and the PDF of SNR in (57), the outage probability is re-expressed as follows

$$\begin{aligned} P_{out,l} &= \frac{1}{\Gamma(\omega_l)} \left(\frac{LN_t D_l^v}{\gamma \eta_l}\right)^{\omega_l} \\ &\times \int_0^{\gamma \eta_l} \gamma_l^{\omega_l-1} \exp\left(-\frac{LN_t D_l^v}{\gamma \eta_l} \gamma_l\right) d\gamma_l \end{aligned} \quad (69)$$

When $\{\omega_l\} \in \mathbb{Z}$, we apply the integral identity [21, eq. (3.351.1)]

$$\int_0^v x^n \exp(-\mu x) dx = \frac{n!}{\mu^{n+1}} - \exp(-u\mu) \sum_{k=0}^n \frac{n! \mu^k}{k! \mu^{n-k+1}} \quad (70)$$

After some simplifications, we can obtain the result of (41).

When $\{\omega_l\} \notin \mathbb{Z}$, we introduce the integral identity [21, eq.(3.381.1)]

$$\int_0^u x^{v-1} \exp(-\mu x) dx = \mu^{-v} \gamma(v, \mu u) \quad (71)$$

After some algebraic manipulations, we can obtain the result of (42). Then, we conclude the proof.

ACKNOWLEDGMENT

The authors would like to thank the associate editor as well as the anonymous reviewers for their constructive comments. Dr. Michail Matthaiou is also greatly acknowledged for his guidance and suggestions.

REFERENCES

[1] A. Sanderovich, S. Shamai (Shitz), and Y. Steinberg, "Distributed MIMO receiver-achievable rates and upper bounds," *Trans. Inf. Theory*, vol. 55, no. 10, pp. 4419–4438, Oct. 2009.
 [2] M. Matthaiou, C. Zhong, M. R. McKay, and T. Ratnarajah, "Sum rate analysis of ZF receivers in distributed MIMO systems," *IEEE J. Sel. Areas Commun.*, vol. 31, no. 2, pp. 180–191, Feb. 2013.

[3] X. Li, J. Wang, L. Li, and C. C. Cavalcante, "Capacity bounds on the Ergodic capacity of distributed MIMO systems over \mathcal{K} fading channels," *KSI Trans. Int. Inf. Syst.*, vol. 10, no. 7, pp. 2992–3009, Jul. 2016.
 [4] X. Li, L. Li, X. Su, Z. Wang, and P. Zhang, "Approximate capacity analysis for distributed MIMO systems over generalized- \mathcal{K} fading channels," in *Proc. Wireless Commun. Netw. Conf. (WCNC)*, vol. 3, Mar. 2015, pp. 241–246.
 [5] H. Suzuki, "A statistical model for urban multipath propagation," *IEEE Trans. Commun.*, vol. 21, no. 25, pp. 673–680, Mar. 1977.
 [6] M. K. Simon and M. S. Alouini, *Digital Communication Over Fading Channels: A Unified Approach to Performance Analysis*, 2nd ed. Hoboken, NJ, USA: Wiley, 2005.
 [7] A. Abdi and M. Kaveh, "K distribution: An appropriate substitute for Rayleigh/lognormal distribution in fading shadowing wireless channels," *Electron. Lett.*, vol. 34, no. 9, pp. 851–852, Apr. 1998.
 [8] T. K. Sarkar, Z. Ji, K. Kim, A. Medouri, and M. Salazar-Palma, "A survey of various propagation models for mobile communication," *IEEE Antennas Propag. Mag.*, vol. 45, no. 3, pp. 51–82, Jun. 2003.
 [9] J. Salo, L. Vuokko, H. M. El-Sallabi, and P. Vainikainen, "An additive model as a physical basis for shadow fading," *IEEE Trans. Veh. Technol.*, vol. 56, no. 1, pp. 13–26, Jan. 2007.
 [10] I. M. Kostic, "Analytical approach to performance analysis for channel subject to shadowing and fading," *IEE Proc. Commun.*, vol. 152, no. 6, pp. 821–827, Dec. 2005.
 [11] D. A. Gore, R. W. Heath, Jr., and A. Paulraj, "Transmit selection in spatial multiplexing systems," *IEEE Commun. Lett.*, vol. 6, no. 1, pp. 491–493, Nov. 2002.
 [12] M. Matthaiou, D. Nestor, and G. K. Karagiannidis, "On the sum rate of ZF detectors over correlated \mathcal{K} fading MIMO channels," in *Proc. IEEE Int. Conf. Coust. Speech Signal Process. (ICASSP)*, May 2011, pp. 3244–3247.
 [13] M. Matthaiou, N. D. Chatzidiamantis, G. K. Karagiannidis, and J. A. Nossek, "ZF detection over correlated \mathcal{K} fading MIMO channels," *IEEE Trans. Commun.*, vol. 59, no. 6, pp. 1591–1603, Jun. 2001.
 [14] M.-J. Ho and G. L. Stuber, "Capacity and power control for CDMA microcells," *ACM J. Wireless Net.*, vol. 1, no. 3, pp. 355–363, Oct. 1995.
 [15] S. Al-Ahmadi and H. Yanikomeroglu, "On the approximation of generalized- \mathcal{K} distribution by a Gamma distribution for modeling composite fading channels," *IEEE Trans. Wireless Commun.*, vol. 9, no. 2, pp. 706–713, Feb. 2012.
 [16] L. Lu, G. Y. Li, A. L. Swindlehurst, A. Ashikhmin, and R. Zhang, "An overview of massive MIMO: Benefits and challenges," *IEEE J. Sel. Topics Signal Process.*, vol. 8, no. 5, pp. 742–758, Oct. 2014.
 [17] F. Boccardi, R. W. Heath, Jr., A. Lozano, T. L. Marzetta, and P. Popovski, "Five disruptive technology directions for 5G," *IEEE Commun. Mag.*, vol. 52, no. 2, pp. 74–80, Feb. 2014.
 [18] X. Li, L. Li, L. Xie, X. Su, and P. Zhang, "Performance analysis of 3D massive MIMO cellular systems with collaborative base station," *Int. J. Antennas Propag.*, vol. 2014, no. 614061, pp. 1–12, Jul. 2014.
 [19] X. Li, L. Li, and L. Xie, "Achievable sum rate analysis of ZF receivers in 3D MIMO systems," *KSI Trans. Int. Inf. Syst.*, vol. 8, no. 4, pp. 1368–1389, Apr. 2014.
 [20] W. R. Heath, Jr., M. Kountouris, and T. Bai, "Modeling heterogeneous network interference using poisson point processes," *IEEE Trans. Signal Process.*, vol. 61, no. 16, pp. 4114–4126, Dec. 2005.
 [21] I. S. Gradshteyn and I. M. Ryzhik, *Table of Integrals, Series, and Products*, 7th ed. San Diego, CA, USA: Academic, 2007.
 [22] M. Chiani, M. Z. Win, and A. Zanella, "On the capacity of spatially correlated MIMO Rayleigh-fading channels," *IEEE Trans. Inf. Theory*, vol. 49, no. 10, pp. 2363–2371, Oct. 2003.
 [23] J. G. Proakis, *Digital Communications*, 4th ed. New York, NY, USA: McGraw-Hill, 2001.
 [24] G. Yang, M.-A. Khalighi, S. Bourennane, and Z. Ghassemloooy, "Approximation to the sum of two correlated gamma-gamma variates and its applications in free-space optical communications," *IEEE Wireless Commun. Lett.*, vol. 1, no. 6, pp. 621–624, Dec. 2012.
 [25] K. P. Peppas, "A simple, accurate approximation to the sum of gamma-gamma variates and applications in MIMO free-space optical systems," *IEEE Photon. Technol. Lett.*, vol. 23, no. 13, pp. 839–841, Jul. 2011.
 [26] M. Evans, N. Hastings, and B. Peacock, *Statistical Distributions*, 2nd ed. New York, NY, USA: Wiley, 2000.
 [27] S. Verdú, "Spectral efficiency in the wideband regime," *IEEE Trans. Inf. Theory*, vol. 48, no. 6, pp. 1319–1343, Jun. 2002.

[28] M. Abramowitz and I. A. Stegun, *Handbook of Mathematical Functions With Formulas, Graphs, and Mathematical Tables*, 9th ed. New York, NY, USA: Dover, 1970.

[29] T. L. Marzetta, "Noncooperative cellular wireless with unlimited number of BS antennas," *IEEE Trans. Wireless Commun.*, vol. 9, no. 11, pp. 3590–3600, Nov. 2010.

[30] M.-S. Alouini and A. J. Goldsmith, "Capacity of Rayleigh fading channels under different adaptive transmission and diversity-combining techniques," *IEEE Trans. Veh. Technol.*, vol. 48, no. 4, pp. 1165–1181, Jun. 1999.

[31] A. P. Prudnikov, Y. A. Brychkov, and O. I. Marichev, *Table of Integrals Volume 1 Elementary Functions*, 4th ed. Overseas Publishers, 1998.

[32] R. Beals and R. Wong, *Special Functions Cambridge Studies in Advanced Mathematics*. Cambridge, U.K.: Cambridge Univ. Press, 2010.

[33] *The Wolfram Functions Site*. [Online]. Available: <http://function-wolfram.com>

[34] T. Eng and L. B. Milstein, "Coherent DS-CDMA performance in Nakagami multipath fading," *IEEE Trans. Commun.*, vol. 43, no. 4, pp. 1134–1143, Feb. 1995.



XINGWANG LI received the B.Sc. degree in communication engineering from Henan Polytechnic University, Jiaozuo China, in 2007, the M.Sc. degree from the National Key Laboratory of Science and Technology on Communications, University of Electronic Science and Technology of China, in 2010, and the Ph.D. degrees in communication and information system from the State Key Laboratory of Networking and Switching Technology at Beijing University of Posts and Telecommunications in 2015. He is currently a Lecturer with the School of Physics and Electronic Information Engineering, Henan Polytechnic University. His research interests include, massive MIMO, hardware constrained communication, physical layer security, NOMA, FSO communications, and the performance analysis of fading channels.



XUEQING YANG received the B.Sc. degree in electronic science and technology from Xinyang Normal University in 2015. She is currently pursuing the M.Sc. degree in communication and information systems with the School of Physics and Electronic Information Engineering, Henan Polytechnic University. Her research interests include massive MIMO and the performance analysis of fading channels.



LIHUA LI received the Ph.D. degree from the Beijing University of Posts and Telecommunications (BUPT), in 2004. She has served as a Group Leader in 3GPP LTE RAN1 standardization on behalf of BUPT in 2005, when she submitted over 20 relevant proposals to 3GPP LTE and seven of them were accepted. She had been a Short-Term Visiting Scholar with Brunel University, U.K., in 2006. She has been taken part with the China IMT-Advanced Technology Work Group, since 2007.

She visited the University of Oulu from 2010 to 2011. She is currently an Associate Professor with BUPT. She has authored 63 papers in international and domestic journals and academic conferences, and five books. She has applied 20 national invention patents and one international patent. She has submitted 33 relevant proposals, 15 of which were accepted. Her research focuses on wideband mobile communication technologies including MIMO, link adaptation, and cooperative transmission technologies relating to new generation mobile communication systems, such as LTE and IMT-Advanced. She received the second prize of the China State Technological Invention Award (the First level award in China) in 2008 and the first prize of the China Institute of Communications Science and Technology Award in 2006 for her research achievements of Wideband Wireless Mobile TDD-OFDM-MIMO Technologies. She was selected and funded as one of the New Century Excellent Talents by the Chinese Ministry of Education in 2008.



JIN JIN received the Ph.D. degree in communications and information systems from the Beijing University of Posts and Telecommunications, Beijing, China, in 2014. Since 2014, he has been with the School of Information Engineering, Zhengzhou University, where he is currently a Lecturer. His research interests include cooperative communications and interference alignment.



NING ZHAO received the B.Sc. degree in communication engineering from Henan Polytechnic University, Jiaozuo, China, in 2005, and the M.Sc. and Ph.D. degrees from the Chengdu University of Technology. He is currently a Lecturer with the Department of Physics and Electronic Information, Henan Polytechnic University. His research interests include electromagnetic simulation and tomography.



CHANGSEN ZHANG received the B.S. degree from Northeast University, China, in 1992, and the Ph.D. degree from the China University of Mining and Technology in 2003. He is currently a Full Professor and the Ph.D. Tutor of Telecommunications with the Department of Communication and Information System, Henan Polytechnic University. He is an Outstanding Young Science and Technology Expert in Jiaozuo and serves as an Academic Leader of Information and Communication Engineering in Henan. His main research interests include wireless sensor network, modern communications technology, and wireless networks' protocols. He was a recipient of the Provincial Science and Technology Progress Award.

...